DECENTRALIZED CONTROL OF AN ACTIVATED SLUDGE PROCESS VIA MODERN PID TUNING TECHNIQUES WITH GUARANTEED STABILITY MARGINS

A Thesis

by

TUSHAR DUTT MATHUR

Submitted to the Office of Graduate and Professional Studies of
Texas A&M University
in partial fulfillment of the requirements for the degree of

MASTER OF SCIENCE

Chair of Committee,	Shankar P. Bhattacharyya
Co-Chair of Committee,	Aniruddha Datta
Committee Members,	Srinivas Shakkottai
	Xingmao "Samuel" Ma
Head of Department,	Miroslav M. Begovic

December 2018

Major Subject: Electrical Engineering

ABSTRACT

In this research, the decentralized control of an Activated Sludge Process (ASP) with the modern Proportional-Integral Derivative (PID) controller tuning techniques is discussed. This tuning technique provides the entire closed loop stabilizing set for a dynamic process. Recent extensions in this algorithm are used to find stability margins feasible from the stabilizing set. The ASP model considered here is a multivariable four-state non-linear model and is linearized to a Two Input Two Output process for control purposes. The input-output pairs are selected by ignoring interactions in the process and the controllers are tuned for these individual control loops. The designed controllers are simulated with the additive process interactions and with the nonlinear model to discuss the effects on designed closed loop stability margins.

The closed loop stabilizing sets are obtained, and the necessary design requirements are specified. Frequency responses for models with and without interactions, and with the non-linear model are compared to validate the design. The models are also subjected to the disturbances to check the performance of controllers. Finally, the design is compared to a multivariable controller to show advantages of using this design methodology for this process.

ACKNOWLEDGEMENTS

I would like to thank my committee chair, Dr. Shankar P. Bhattacharyya, and my committee members, Dr. Aniruddha Datta, Dr. Srinivas Shakkottai, and Dr. Xingmao "Samuel" Ma, for their guidance and support throughout the course of this research. I would also like to thank Sangjin Han for providing valuable inputs.

Thanks also go to the department faculty and staff for making my time at Texas A&M University a great experience.

Finally, thanks to my mother, father and my brother for their encouragement.

CONTRIBUTORS AND FUNDING SOURCES

Contributors

This work was supervised by a thesis committee consisting of Dr. Shankar P. Bhattacharyya, Dr. Aniruddha Datta, and Dr. Srinivas Shakkottai of the Department of Electrical and Computer Engineering, and Dr. Xingmao “Samuel” Ma of the Department of Civil Engineering.

All work for the thesis was completed independently by the student.

Funding Sources

There are no outside funding contributions to acknowledge related to the research and compilation of this document.

TABLE OF CONTENTS

Page

LIST OF FIGURES

Page

LIST OF TABLES

Page

1. INTRODUCTION AND LITERATURE REVIEW

The Activated Sludge Process (ASP), the most commonly used process in the biological treatment stage in wastewater treatment plants. In this process microorganisms consume the organic pollutant and nutrients present in the primary influent. These microorganisms are suspended in the aeration basin and continuous diffusion of oxygen facilitates their growth. Blowers or diffusers aerate the continuously stirred aeration basin to maintain homogeneous concentrations.

As the microorganisms grow with time, the mixture can move to a second tank, called clarifier, where the floc separates from the liquid phase by settling towards the bottom of the tank with the help of gravity. This allows production of a clear effluent, which is then extracted from the top of the tank. Some of the settled concentrated sludge is recycled back to the aeration tank to maintain an adequate quantity of concentration of these microorganisms and hence a proper food to mass ratio is sustained. The remaining excess sludge is wasted to landfills or as fertilizers.

With the continuous flow, the system experiences a wide variety in composition and concentrations of substrate and dissolved oxygen in the influent. It is necessary that both the pollutants are removed, and a suitable amount of oxygen be present in the water to be considered as treated.

Over the years many different models have been developed for academic research purposes, most notably by the International Water Association [1] and are highly non-linear models with multiple states and contain a lot of parameters with multiple kinetic

constraints. The Activated Sludge Models (ASMs) were designed to help researchers and peers, use the best possible and physically accurate models for training, design, optimization and control purposes. The fig. 1 [2] shows a simplified version of ASP which is being considered in this report for control system design.

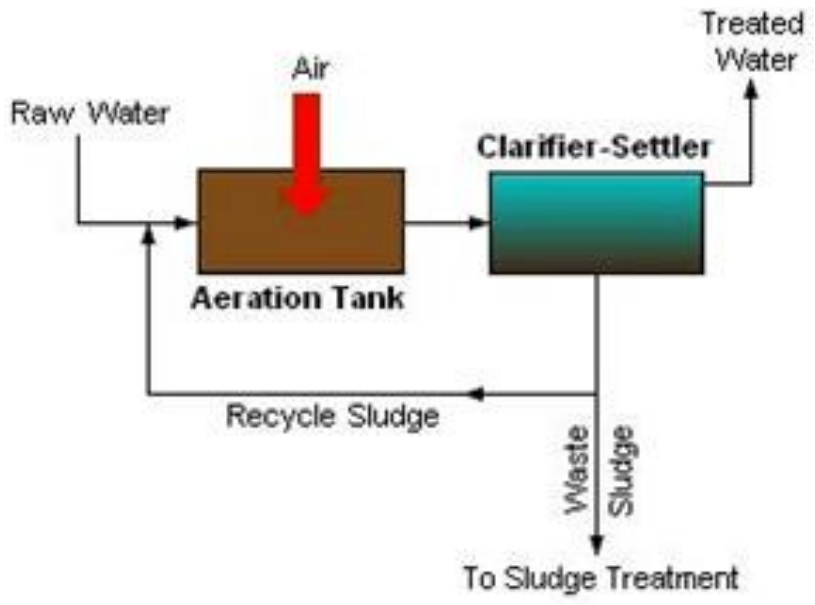

Figure 1. The Activated Sludge Process (Reprinted from Wikimedia Commons)

Previously, this model has been used for implementation of various control strategies like; non-linear multivariable adaptive control using an estimator for estimation of biological states and parameter variables in the process [3], a case study of a plant in Romania and design of decentralized PI controllers using conventional tuning strategies [4], the first order model approximation of the process and decentralized control using multi loop 2-DOF PI controllers [5], a multivariable PID controller which diagonalizes

the system at a wide range of frequencies to eliminate interactions [6] [7], a robust multivariable H∞ Control where the results were discussed for the model with multiple operating conditions and uncertainties [8], and a robust PID controller design using genetic algorithm [9].

There has been plentiful research with decentralized control design with PI/PID controllers for the Activated Sludge Process, but none of them give an idea about the scope of the entire stabilizing set with best achievable stability margins. This paper discusses, a decentralized PID control strategy based on modern results, where the entire closed loop stabilizing set is obtained by using the signature method developed by [10] and after the set has been found, the achievable performance requirements for stability margins by will be specified using the techniques in [11] and [12]. We design the controllers for individual loops of the linearized system and prescribe stability margins at the desired crossover frequency. These controllers are then tested with internal process interactions and with the non-linear model to check if the desired performance is inherited.

2. CONTROL SYSTEM DESIGN

2.1 Process Modeling

Applying mass balance equations on Fig. 1 yields the following set of non-linear differential equations,

$$\dot{X}(t) = \mu(t)X(t) - D(t)(1+r)X(t) + rD(t)X_r(t) \tag{1}$$

$$\dot{S}(t) = -\left(\frac{\mu(t)}{Y}\right)X(t) - D(t)(1+r)S(t) + D(t)S_{in} \tag{2}$$

$$\begin{aligned}\dot{DO}(t) = -K\left(\frac{\mu(t)}{Y}\right)X(t) - D(t)(1+r)DO(t) + D(t)DO_{in} \\ + \alpha W(t)[DO_S - DO(t)]\end{aligned} \tag{3}$$

$$\dot{X}_r(t) = D(t)(1+r)X(t) - D(t)(\beta + r)X_r(t) \tag{4}$$

X(t), S(t), DO(t) and $X_r(t)$ are the biomass, substrate, dissolved oxygen and recycled biomass concentrations respectively. S_{in} and DO_{in} are the substrate and dissolved oxygen concentrations in the influent. *D(t)* - dilution rate (the ratio of influent flow rate to aerated tank's volume), *W(t)* - aeration rate, DO_S - saturation concentration of dissolved oxygen, *Y* - biomass yield factor, α - oxygen transfer rate, *r* - the ratio of recycled sludge flow to influent flow, β - the ratio of waste flow to influent flow and *K* is a constant and μ(t) is the specific biomass growth rate, which relates the microbial growth rate to the available nutrient. It can be modeled using the Monod equation and of the models were suggested by Olsson [13].

$$\mu(t) = \mu_{max}\left(\frac{S(t)}{K_s + S(t)}\right)\left(\frac{DO(t)}{K_{DO} + DO(t)}\right) \quad (5)$$

Where, μ_{max} - maximum specific growth rate, K_s and K_{DO} are rate limiting constants.

Initially S_{in}, and DO_{in} are taken as constant for modeling purposes, but they vary according to the composition of the influent, but changes in them are taken account later in this paper during simulations. The values of model parameters are taken as listed in table 1 [3] and the operating point for the system by setting steady state inputs $D = 0.06\ h^{-1}$ and $W = 80$ l/h as in table 2.

Table 1. Typical values of parameters [3]

$\alpha = 0.018\ m^{-3}$	$DO_S = 10$ mg/l
$\beta = 0.2$	$DO_{in} = 0.5$ mg/l
$r = 0.8$	$S_{in} = 200$ mg/l
$Y = 0.65$	$K_{DO} = 2$ mg/l
$K = 0.5$	$K_S = 100$ mg/l
$\mu_{max} = 0.15\ h^{-1}$	

Table 2. Operating point for linearization

X = 284.88 mg/l
S = 23.45 mg/l
DO = 6.62 mg/l
Xr = 512.79 mg/l

The system is linearized around this point and taking measurements of Substrate and Dissolved oxygen a Two Input Two Output (TITO) process is obtained, which can be expressed in the form:

$$\begin{bmatrix} S \\ DO \end{bmatrix} = \begin{bmatrix} G_{11} & G_{12} \\ G_{21} & G_{22} \end{bmatrix} \begin{bmatrix} D \\ W \end{bmatrix} \tag{6}$$

Or

$$S = G_{11}D + G_{12}W \tag{7}$$

$$DO = G_{21}D + G_{22}W \tag{8}$$

Where,

$$G_{11} = \frac{157.8\,s^3 + 303.6\,s^2 + 46.75\,s + 0.3591}{s^4 + 2.312\,s^3 + 1.021\,s^2 + 0.1135\,s + 0.0006816}$$

$$G_{12} = \frac{-0.0246\,s^2 - 0.004133\,s - 3.188 * 10^{-5}}{s^4 + 2.312\,s^3 + 1.021\,s^2 + 0.1135\,s + 0.0006816}$$

$$G_{21} = \frac{-10.77\,s^3 - 30.36\,s^2 - 4.81\,s - 0.02695}{s^4 + 2.312\,s^3 + 1.021\,s^2 + 0.1135\,s + 0.0006816}$$

$$G_{22} = \frac{0.06725\,s^3 + 0.0391\,s^2 + 0.004757\,s + 2.85 * 10^{-5}}{s^4 + 2.312\,s^3 + 1.021\,s^2 + 0.1135\,s + 0.0006816}$$

2.2 Decentralized Control

The PID controller can only be designed for a Single Input Single Output (SISO) system. The system considered in this thesis is a multivariable Two Input Two Output process (TITO) as in fig. 2, and to get the desired output response by manipulating inputs, a multivariable control strategy should be implemented. But if we were to select input output pairs, a PID controller can be implemented for each process. Hence, effectively converting a TITO process to two SISO loops. This strategy is called Decentralized Control. Decentralized control is implemented because it requires minimum modeling effort for control design, and is relatively easier to understand from the operator's point of view [14].

In such a strategy, the system is effectively diagonalized by using de-couplers or compensators. The measure of interactions from off-diagonal elements also of importance as a system with larger interactions is difficult to de-couple and choosing input output pairs for control may not give the desired performance. If the interaction measure from off-diagonal elements is low and does not have a significant impact on the dynamics of the system, then a robust controller like PID does not need a de-coupler to compensate any interactions for good performance.

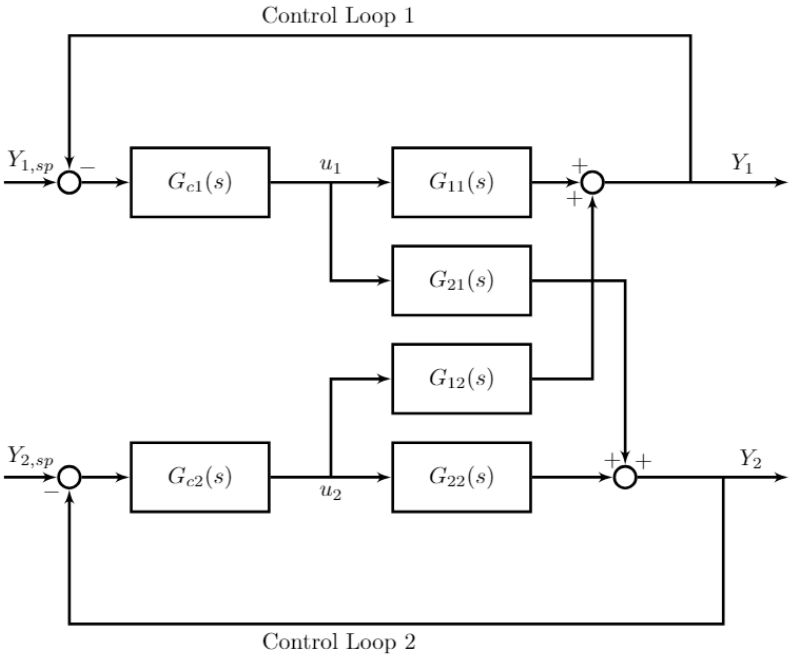

Figure 2. Closed loop TITO process

2.3 Relative Gain Array analysis

The Relative Gain Array (RGA) is analyzed for the measure of interaction in a multivariable system at the steady state [15] and has also been extended as Dynamic Relative Gain Array (DRGA) for all frequencies. DRGA can be calculated as follows:

$$RGA(G) = G(i\omega) \text{o} (G^{-1}(i\omega))^T \tag{9}$$

Where, o denotes Hadamard or Schur Product of the two matrices.

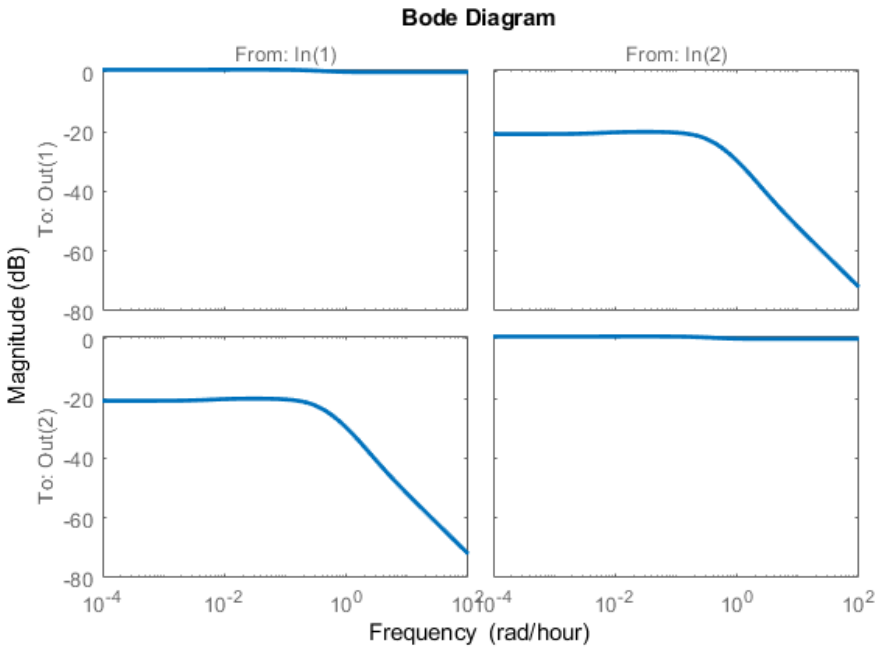

Figure 3. Dynamic Relative Gain Array

RGA is the ratio of gains for each input-output (I/O) pair when the remaining I/O pair loops are open to when all the remaining I/O pair loops are closed. Gains closest to 1 indicate good affinity in I/O pair. The input output pairing selected should correspond to the value which is closest to 1. Fig. 3 shows RGA for ASP at all frequencies.

For frequencies greater than 1 rad/hour, the magnitude of off-diagonal elements is very less and at higher frequencies, the system is effectively diagonal, which means that interactions at these frequencies do not severely affect the dynamics of the system. Hence, the pairing substrate (S) with dilution rate (D) and dissolved oxygen (DO) with the aeration rate (W) is chosen and the interactions are ignored while tuning the controllers for these individual loops.

Therefore, we design PID controllers for systems G_{11} & G_{22}, in the equations (7), (8) and assuming $G_{12} = 0$ & $G_{21} = 0$, by treating them as two separate SISO loops. Hence, the control scheme is implemented such that Substrate and Dissolved Oxygen are controlled by inputs Dilution rate and Aeration rate respectively and the controller takes the following form:

$$C = \begin{bmatrix} C_S & 0 \\ 0 & C_{DO} \end{bmatrix} \tag{10}$$

2.4 PID Design

2.4.1 Calculation of Sabilizing Set

This section presents a summary to calculate closed loop stabilizing set for a continuous process without time delay, using the procedure developed in [10].

Suppose the PID controller is of the form:

$$C(s) = \frac{K_d s^2 + K_p\, s + K_i}{s(1 + \tau s\,)} \tag{10}$$

And the plant is given by:

$$P(s) = \frac{N(s)}{D(s)} \tag{11}$$

Then the characteristic equation of the closed loop system is:

$$\delta(s) = s(1 + \tau s\,)D(s) + \left(K_d s^2 + K_p\, s + K_i\right)N(s) \tag{12}$$

Using the characteristic polynomial, the polynomial $\nu(s)$ is defined as:

$$\nu(s) = \delta(s)N(-s) \tag{13}$$

$$\nu(s) = \nu_{even}(s^2, K_i, K_d) + s\nu_{odd}(s^2, K_p) \tag{14}$$

The polynomial $\nu(s)$ exhibits that K_p appears only in the odd part of the polynomial $\nu(s)$ and K_i , K_d only appear in the even part of $\nu(s)$ as seen in the equation (14). This will enable the computation of the stabilizing set using signature concepts.

Let deg[D(s)] = *m*, and deg[N(s)] = *n* and let z^+ and z^- denote the number of Right Half Plane and Left Half Plane zeros of the plant, respectively, that is, zeros of $N(s)$. It is assumed, for technical convenience, that the plant has no *j*ω axis zeros. Then the closed loop system will be stable if and only if:

$$\sigma(\nu) = n - m + 2 + 2z^+ \tag{15}$$

where, $\sigma(\nu)$ is the signature number of the polynomial $\nu(s)$.

Based on this, the following steps are used to calculate the closed loop stabilizing set:

- Fix $K_p = K_p^*$ and let $0 < \omega_1 < \omega_2 < \cdots < \omega_{l-1}$ denote the real, positive, finite frequencies which are zeros of

$$\nu_{odd}(-\omega^2, K_p^*) = 0 \tag{16}$$

of odd multiplicities. Let $\omega_0 := 0 \; and \; \omega_l := \infty$.

- Write $j = sgn\left[v_{odd}\left(0, K_p^*\right)\right]$ and determine strings of integers $i_0, i_1, \ldots$ such that:

  If $n + m$ is even:

$$j(i_0 - 2i_1 + 2i_2 + \cdots + (-1)^{l-1}2i_{l-1} + (-1)^l i_l) = n - m + 2 + 2z^+ \qquad (17)$$

  If $n + m$ is odd:

$$j(i_0 - 2i_1 + 2i_2 + \cdots + (-1)^{l-1}2i_{l-1}) = n - m + 2 + 2z^+ \qquad (18)$$

- Let $I_1, I_2, I_3, \ldots$ denote diverse strings $\{i_0, i_1, \ldots\}$ which satisfy the expression in (17) or (18). Then the stabilizing sets in K_i, K_d space, for $K_p = K_p^*$ are given by the linear inequalities:

$$v_r(-\omega_t^2, K_i, K_d)i_t > 0 \qquad (19)$$

  Where, the i_t range over each of the string $I_1, I_2, \ldots$.

- For each string I_j, the solution of equation (19) creates a convex stability set $S_j\left(K_p^*\right)$ and the complete set for fixed K_p^* is the union of these convex sets:

$$S\left(K_p^*\right) = \cup_j S_j\left(K_p^*\right) \qquad (20)$$

- The complete stabilizing set in $\left(K_p, K_i, K_d\right)$ space can be found by repeating the steps above for all feasible values of K_p over the real axis.

2.4.2 Constant Gain and Phase Loci

This section presents a summary to design the PID controller in the achievable margin plane using the procedure developed in [11] and [12].

Let the equations (10) and (11) represent the controller and plant transfer functions respectively. Then in frequency domain:

$$C(j\omega) = \frac{K_d(j\omega)^2 + K_p\,(j\omega) + K_i}{j\omega(1 + \tau(j\omega)\,)} \tag{21}$$

$$P(j\omega) = \frac{N(j\omega)}{D(j\omega)} \tag{22}$$

Then at prescribed closed loop gain crossover frequency:

$$\left|P(j\omega_g)C(j\omega_g)\right| = 1 \tag{23}$$

$$\left|C(j\omega_g)\right| = \frac{1}{\left|P(j\omega_g)\right|} = M_g \tag{24}$$

$$\phi_g = \pi + pm - \angle P(j\omega_g) \tag{25}$$

Therefore,

$$\left|C(j\omega_g)\right|^2 = M_g^2 \tag{26}$$

$$\arg[C(j\omega_g)] = \tan\phi_g \tag{27}$$

Solving equations (26) and (27) for the desired ω_g will give constant gain loci cylinder and constant phase loci plane *in* K_p, K_i, K_d space.

The corresponding points of design which attain the prescribed specification are the intersection of these loci lies in the stabilizing set. If there is no intersection of loci with stabilizing set, then the prescribed specification is not achievable.

The detailed calculations for stabilizing sets and prescribing performance margins can be found in Appendix A.

3. RESULTS

Applying the methods discussed in the previous section, stabilizing sets for G_{11} and G_{22} are obtained for the PID controller as in (10). We choose $\tau = 1$ so that the controller can reject noises above 1 rad/hr.

For control loop Substrate from Dilution rate (i.e. for control of G_{11}), the allowable range for proportional gain is $K_p \in (-0.02\,, \infty)$. The fig. 4 shows stabilizing set for values of K_p up to 0.2. Similarly, for control loop Dissolved oxygen from aeration rate (i.e. for control of G_{22}), the allowable range for proportional gain is $K_p \in (-20\,, \infty)$. The fig. 5 shows stabilizing set for values of K_p up to 100.

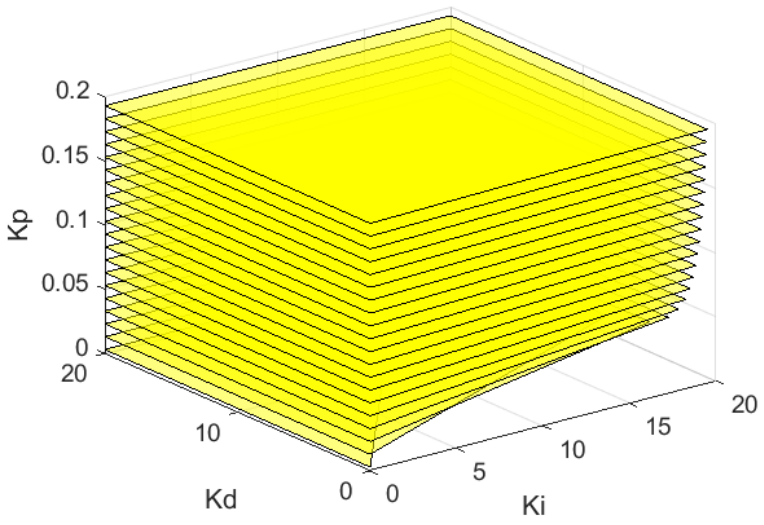

Figure 4. Stabilizing set for loop 1 (Substrate)

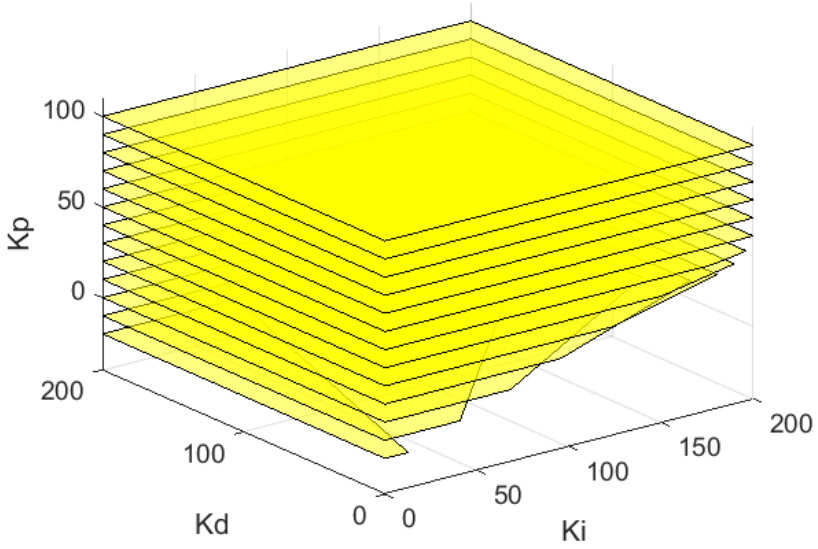

Figure 5. Stabilizing set for loop 2 (Dissolved Oxygen)

For design specifications, the crossover frequencies are only prescribed above $1\,rad/hr$ as the magnitude of interactions is negligible as seen in the RGA analysis section. Also, the system should be able to attenuate variations with a period larger than 2 hours [16]. Hence, we choose the design point such that $\omega_g = 2\,rad/hr$ and $PM = 60^o$ for both control loops. The fig. 6 and 7 show the intersection of stabilizing set with constant phase and gain loci in equations (26) and (27). The design point is chosen from this line of intersection, if it lies in the stabilizing set, to get the controller gains for desired specifications.

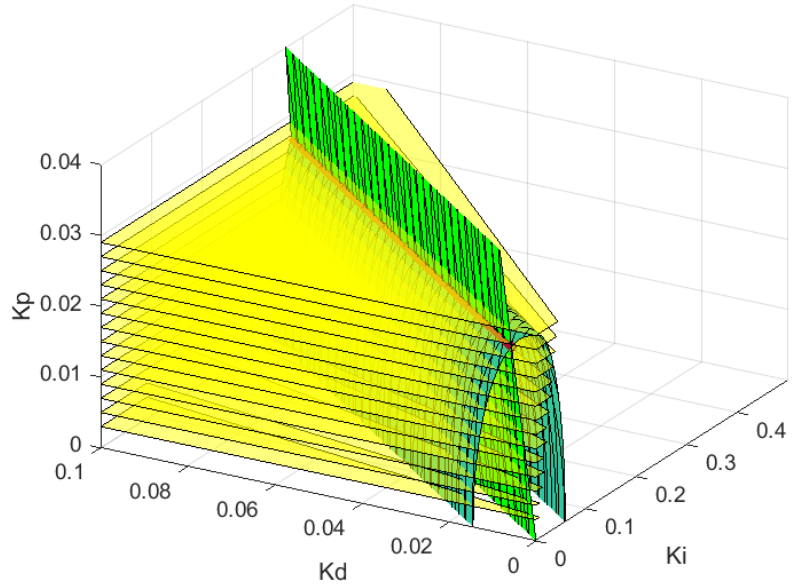

Figure 6. Intersection of loci with stabilizing set (Red line) for loop 1

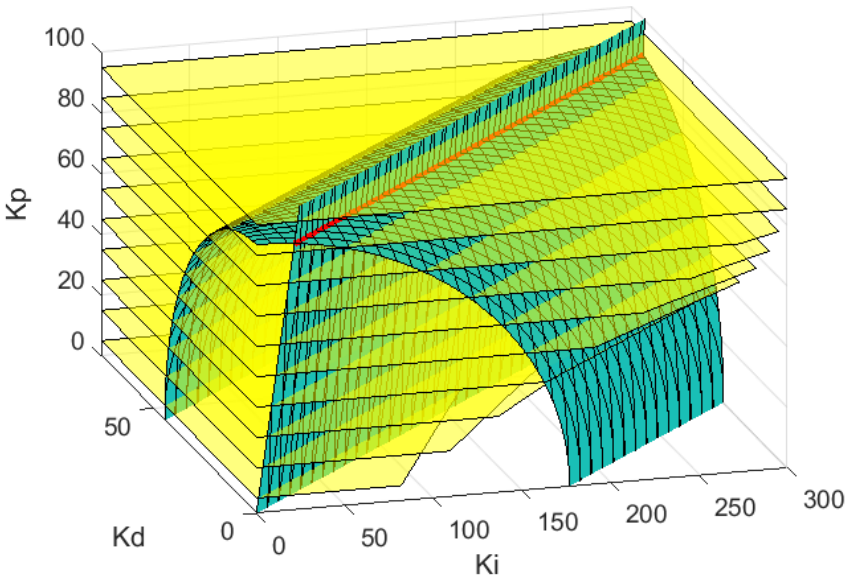

Figure 7. Intersection of loci with stabilizing set (Red line) for loop 2

The design point is chosen with low values of K_i and K_d so that we can get a low value of overshoot and better settling time. Hence, the controllers are:

$$C_S(s) = \frac{0.00806s^2 + 0.02672s + 0.01}{s(1+s)} \tag{28}$$

$$C_{DO}(s) = \frac{0.1286s^2 + 87.85s + 22}{s(1+s)} \tag{29}$$

3.1 Response with Linearized Model

The fig. 8 shows the step response of the system. The designed controllers provide a good response for the respective control loops and with off-diagonal interaction terms decaying to zero.

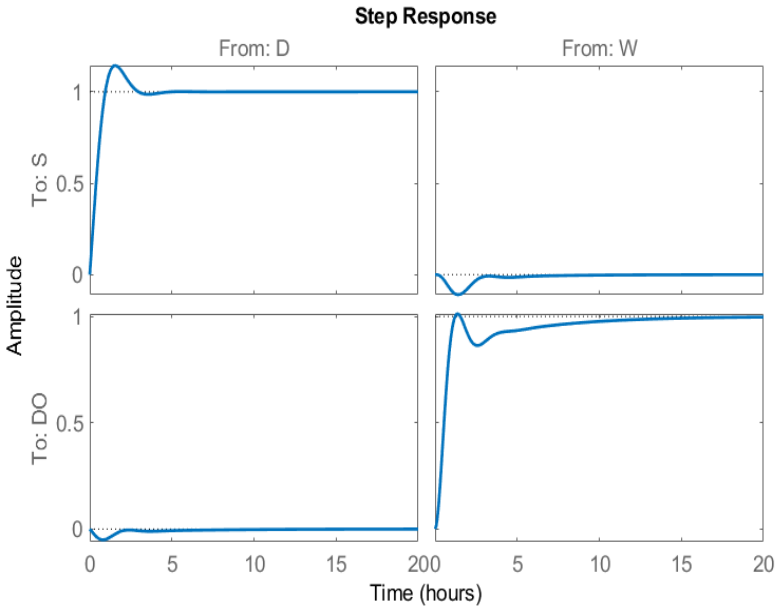

Figure 8. Step Response of S and DO to inputs with designed controllers

The model in fig. 9 was developed in MATLAB Simulink, using the controllers designed in the previous section to simulate the closed loop TITO process.

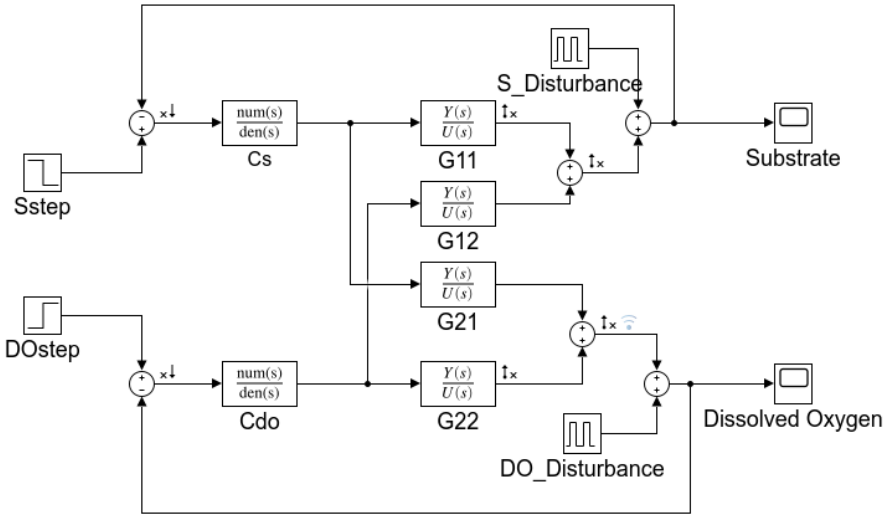

Figure 9. Closed loop TITO process in MATLAB Simulink

The simulated response for a set point change from 45 mg/l to 55 mg/l for Substrate concentration at *t = 50 hours* and set point change from 4.5 mg/l to 6 mg/l for Dissolved oxygen at *t = 75 hours* is shown in fig. 10 along with the inputs required to the system to track these setpoints.

The system response when a periodic disturbance of 10 mg/l every 24h and 0.5 mg/l every 12h is added in the S and DO loops respectively is shown in fig. 11. The disturbance in S and DO loops is eliminated by manipulating the inputs, dilution and aeration rates respectively.

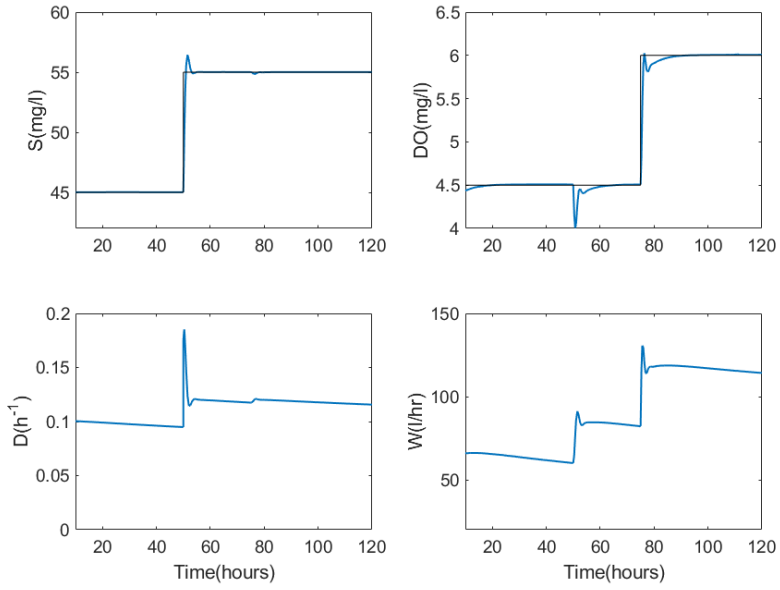

Figure 10. Simulation of TITO process with reference signal (solid-red) for linearized model (solid-blue)

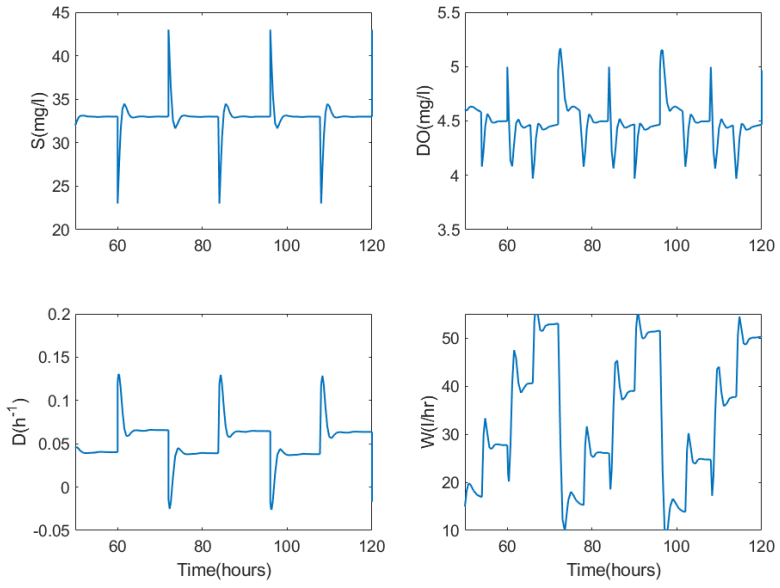

Figure 11. Effect of periodic disturbances in control loops

The bode plots for the loops with and without interactions are obtained by setting linear analysis points on the connections before and after additive interaction connection for both loops and are shown in fig. 12 and 13. By analyzing bode plots, we can check if these interactions have any effect the desired performance. As discussed previously, the effect of the interactions is higher in frequencies below 1 rad/hour. Therefore, the system inherits designed performance specifications for the chosen crossover frequency for both loops.

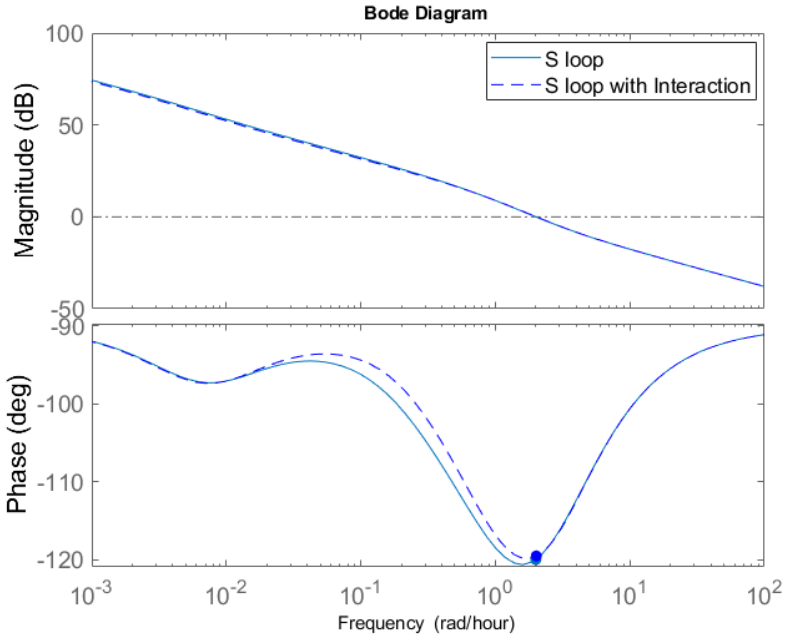

Figure 12. Bode plot of S loop function with (dashed) and without interaction (solid)

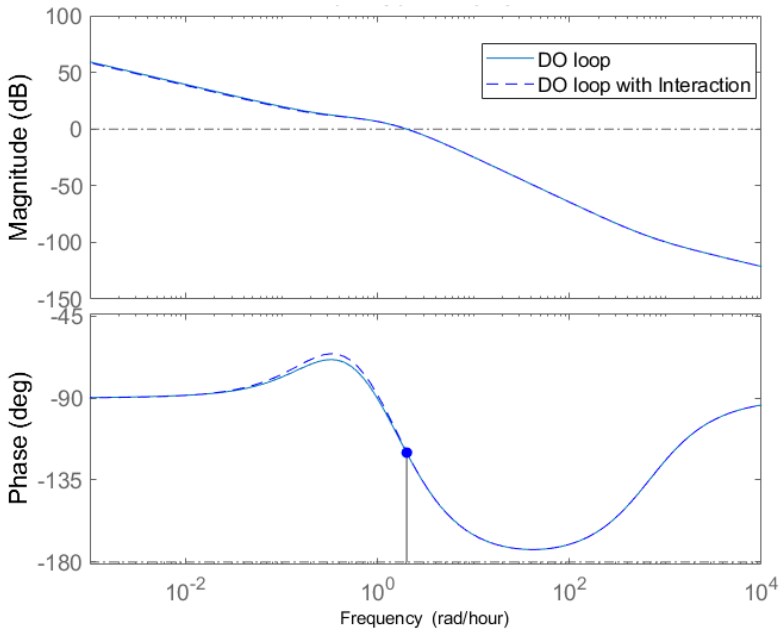

Figure 13. Bode plot of DO loop function with (dashed) and without interaction (solid)

The Gain margin that can be achieved for this design is infinite for both the loops and has a Phase margin of 60 degrees at the gain crossover frequency of 2 rad/hour, equal to the initial design point for loops with no interactions.

3.2 Response with Non-Linear Model

The model in fig. 14 shows the non-linear process designed in MATLAB Simulink and the previously designed controllers are implemented for the closed loop process. The closed loop simulated response is shown in fig. 15.

It is observed that the designed controllers work well for the non-linear system to with good performance. The setpoint change for S occurs at *t = 50 hours* and for DO at *t = 75 hours*. The dynamics of oxygen are affected by the increase in concentration of

substrate at 50-hour mark and would cause concentration of dissolved oxygen to decrease as the demand of oxygen increase as there are more pollutants to oxidize.

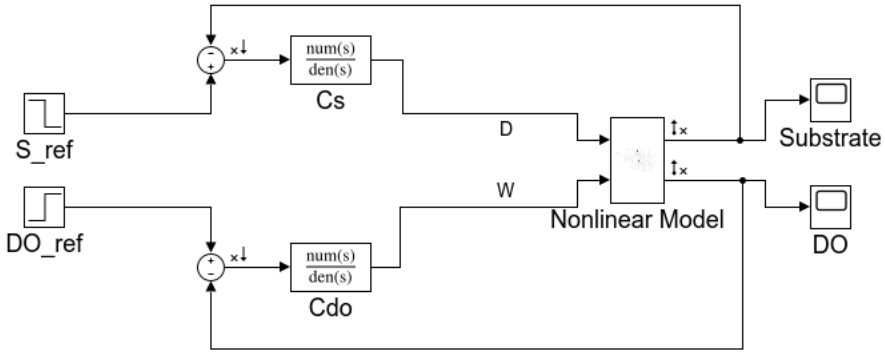

Figure 14. Closed loop model with non-linear plant

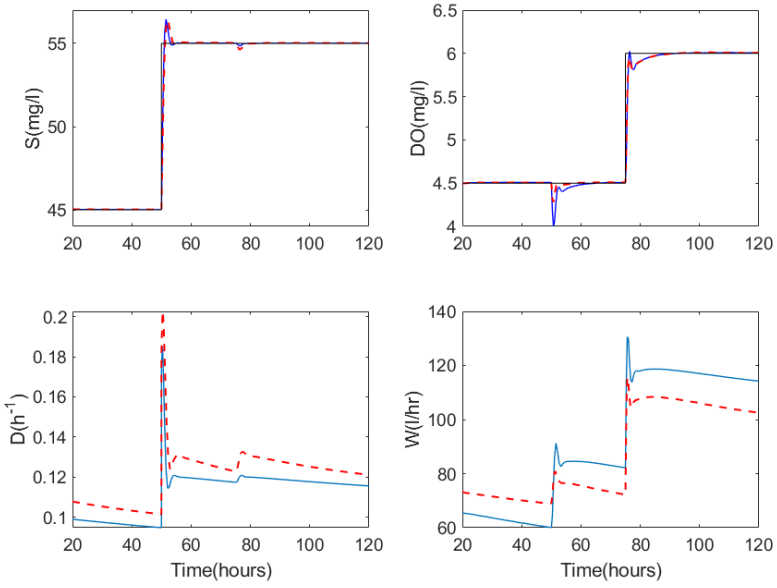

Figure 15. Closed loop response for the reference signal (solid-black) with non-linear model (dashed-red) compared to linearized model (solid-blue)

Around 75-hour mark the concentration of substrate dips due to increase in the concentration of DO at setpoint change. To compensate this, there is a slight increase in dilution rate to get the substrate concentration back up to desired value. It should also be noted that there is a difference in control effort required for the linear and non-linear plant because of difference in dynamics.

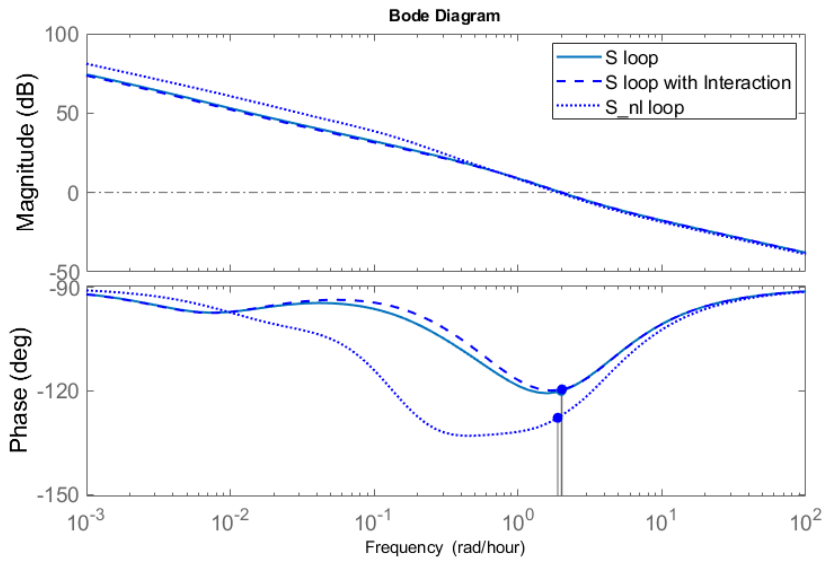

Figure 16. Bode plot of S loop function with (dashed), without interaction (solid) and non-linear model (dotted)

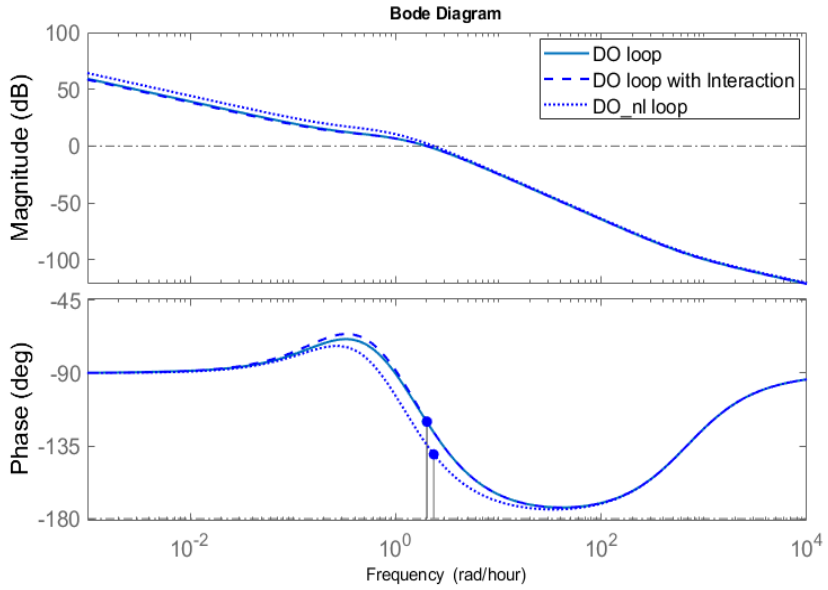

Figure 17. Bode plot of DO loop function with (dashed), without interaction (solid) and non-linear model (dotted)

It is seen that there is a decrease in phase margins in both loops. For the Substrate control loop it is about 52 degrees at 1.9 rad/hr and for DO control loop it is 40 degrees at 2.3 rad/hr as shown in fig.16 and 17. The loops in non-linear systems do not exactly inherit the exact performance designed for the controllers, but they do have a sufficient amount of margins near the prescribed crossover frequency. It should also be noted that for an interactive system, it is only as stable as the least stable loop.

For DO loop, delay margin decreases from 0.52 hours to 0.36 hours and this is an important metric as there are time delays in such a treatment plant from the valve opening to oxygen transfer to saturation in the tank [17]. Several factors may affect the diffusion of oxygen into the influent, like the weather, viscosity of sludge, pH level, etc., and if the diffusion time crosses this delay margin, the desired value of oxygen is not obtained, and

it is necessary that a sufficient amount of oxygen be present in the effluent to be considered as treated according to industry standards. Hence, it is necessary that large margins are designed to take issues like this into account.

It was initially assumed that substrate and dissolved oxygen concentrations in the influent are constant. The robustness of the controller designed can be tested by varying S_{in} and DO_{in} values. The S_{in} and DO_{in} are varied by 10% every 24h and 12h respectively. It is observed that, the designed controllers provide good performance for this uncertainty when simulated with the non-linear model.

This uncertainty is eliminated by manipulating the dilution and aeration rates as seen in fig. 18. This means that when S_{in} concentration increases by 10% of its initial value, the equilibrium of the substrate and sludgle concentration is disturbed and to compensate this, the dilution rate decreases so that microbial population can grow quicker than inlet substrate to attain equilibrium. For any increase/decrease in the inlet DO concentration, the aeration rate will decrease/increase to maintain the desired concentration.

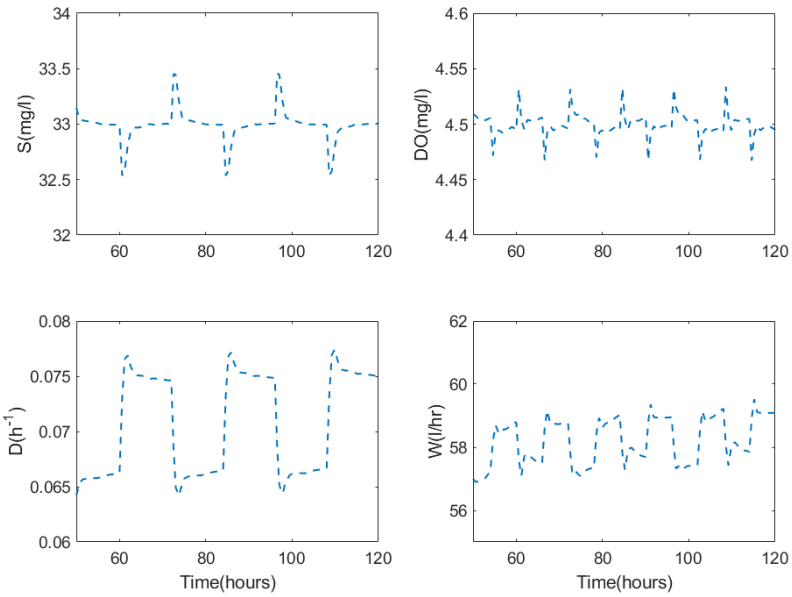

Figure 18. Response of non-linear model with uncertainty in input substrate and dissolved oxygen concentration

Since there is a decrease in margins when the designed controllers are implemented on the nonlinear model. The poorly tuned controllers with very low margins will not give a satisfactory performance. Suppose, the controllers were tuned such that they have PM of 5 degrees at crossover frequency 1.2 rad/hr for both loops. The step response of controllers with the linearized system is shown in fig. 19. The response is oscillatory, but it is decaying. When the same controllers are used in closed loop simulation with nonlinear system, the response becomes unstable and does not decay, as shown in fig. 20. This oscillatory behavior is undesirable and will damage the actuators and the quality of effluent will be compromised.

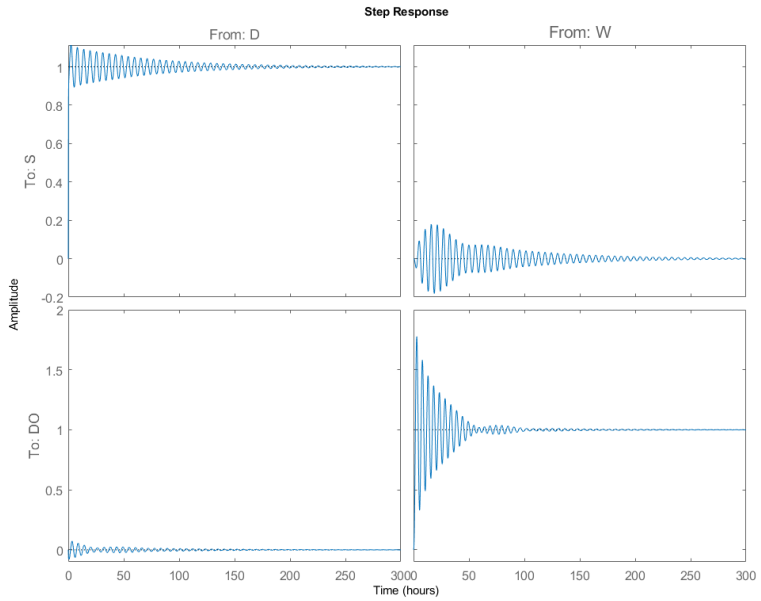

Figure 19. Step response of linearized model with poor controller design

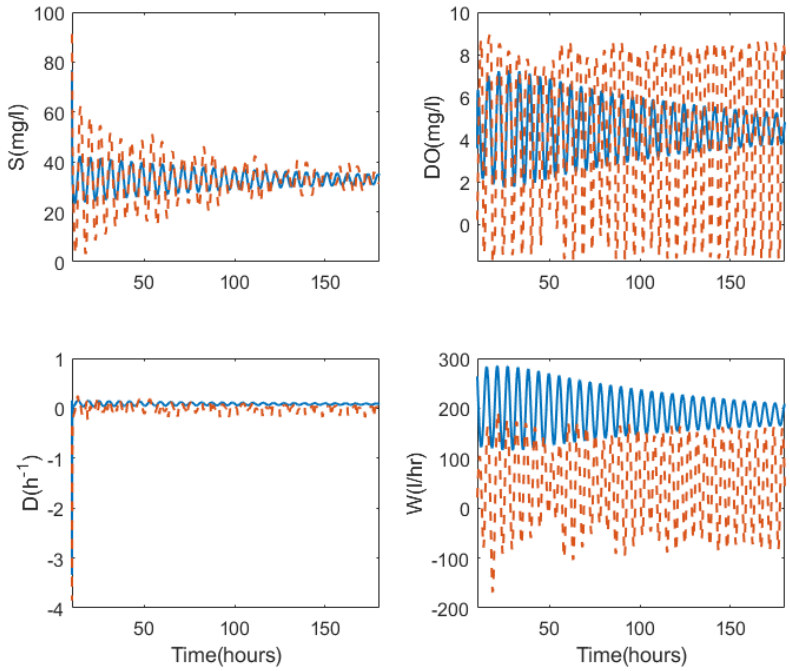

Figure 20. Closed loop response with non-linear model (dashed-red) compared to linearized model (solid-blue)

4. COMPARISON WITH MIMO CONTROLLER

The existing literature in control design for this process discusses a few multivariable control techniques [5] [6] [7] [8]. One such technique is compensator design using Maciejowski's method [18], which results in compensator that makes system diagonally dominant at specified bandwidth ω_b, assuming that same bandwidth can be prescribed for all the control loops. Suppose a PI controller:

$$C(s) = K_p + \frac{K_i}{s} \tag{30}$$

Where, $K_p = \rho G^{-1}(j\omega_b)$ and $K_i = \varepsilon G^{-1}(j\omega_b)$. The approximation of $G^{-1}(j\omega_b)$ is computed using ALIGN algorithm [19]. The controller in [5] and [7] is used for comparison purposes in this report.

$$K \approx G^{-1}(j0.02) = \begin{bmatrix} 0.0021 & 0.0033 \\ 1.2955 & 28.67 \end{bmatrix} \tag{31}$$

The scalar tuning parameters were taken $\rho = 1$ and $\varepsilon = 0.312$. The controller here will make the system diagonally dominant at bandwidth 0.02 rad/hr. It was observed that this controller prescribes PM of 87 degrees at 0.3 rad/hr for Substrate control loop and PM of 131 degrees at 1.18 rad/hr for DO control loop and infinite GM for both for the non-linear system. Using modern PID tuning techniques it is possible to get similar margins at

higher crossover frequencies without having to realize and approximate $G^{-1}(j\omega_b)$ by using a complex optimization algorithm. We choose a controller from the stabilizing set and loci such that it prescribes highest achievable PM and GM at crossover frequency 3 rad/hr. The highest achievable PM in Substrate and DO control loops is 90 and 125 degrees respectively with GM being infinite for both loops for the linearized system. This crossover frequency provides a larger bandwidth as compared to the controller presented in the existing literature.

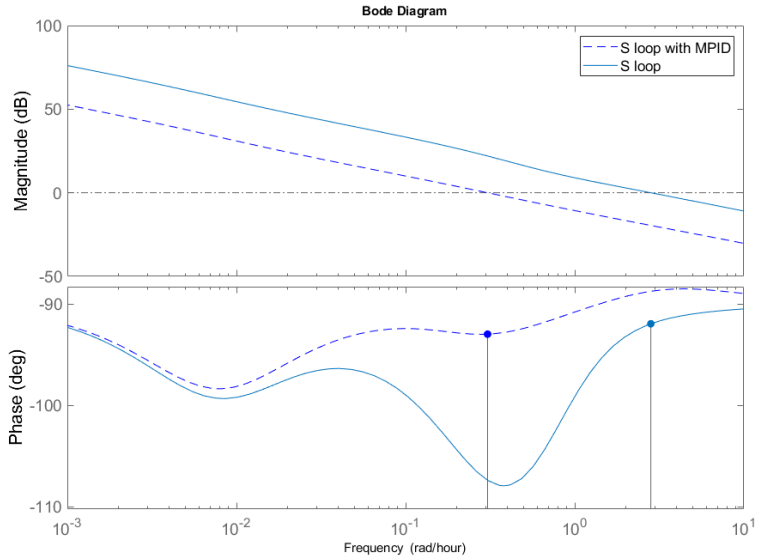

Figure 21. Bode plot of S loop function for Multivariable PID (dashed), and decentralized PID (solid)

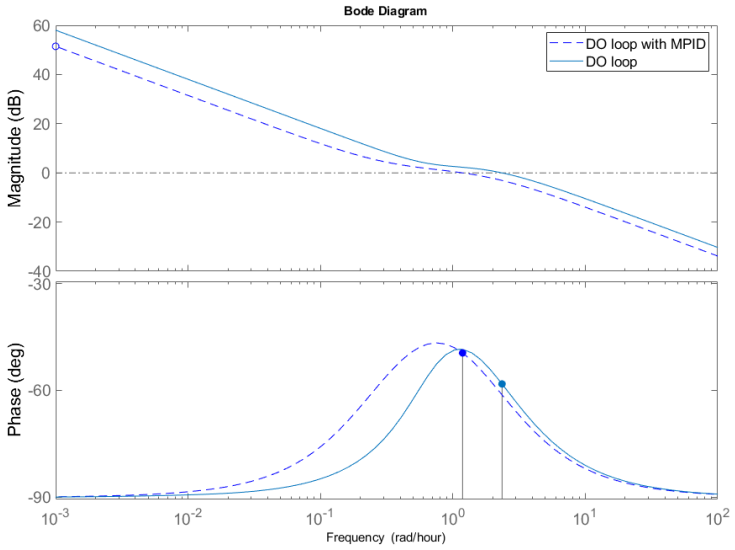

Figure 22. Bode plot of DO loop function for Multivariable PID (dashed), and decentralized PID (solid)

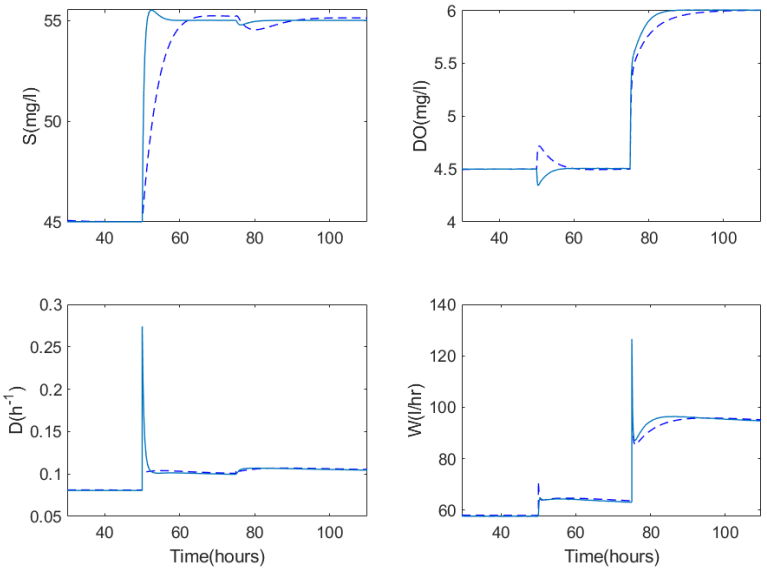

Figure 23. Response of non-linear model with Multivariable PID (dashed), and decentralized PID (solid)

The non-linear system achieves PM of 87 degrees at 2.82 rad/hr and 122 degrees at 2.35 rad/hr for the S and DO loops respectively as seen in fig. 21 and 22. The fig. 23 shows the comparison for both the controllers with setpoints 55 mg/l for substrate and 6 mg/l for DO. As observed, the performance of modern PID is slightly better in terms of settling time than multivariable PID only because a higher bandwidth was achieved. The design of multivariable PID starts with the assumption that same bandwidth can be prescribed for all the control loops in the MIMO process, but in a real-world process, some control loops might require faster times and some slower. The decentralized control strategy and controller tuning process discussed in this report can be advantageous in this aspect as with two different controllers one can prescribe crossover frequencies and bandwidth for a control loop separately.

5. CONCLUSIONS

Applying this modern approach of tuning PID controllers combined with recent results for finding achievable performance gives suitable results for control purposes in an Activated Sludge Process.

The flexibility of tuning the controllers for each process is advantageous in the sense that performance of each loop can be considered independently. Since, the entire stabilizing set for each controller is obtained, it is easy for the operator to implement the controllers without any further calculations.

The margins are designed keeping in mind that every process has variations when operating in real time. Hence, the system will remain stable even if there is an uncertainty in a parameter of the model. If the plant operator expects big uncertainty (like rains or dry weather), then a controller can be tuned with a guarantee of larger margins.

The dynamics of interactions do not have a considerable effect on the control loops in this process. However, the results for the processes where interactions are of higher magnitudes is an area yet to be studied further for concluding anything concrete for decentralized control design using this technique.

REFERENCES

[1] The IWA Task Group on Mathematical Modelling for Design and Operation of Biological Wastewater Treatment, Activated Sludge Models, IWA Publishing, 2000.

[2] LennyCZ, "Activated Sludge 1.svg," 2008. [Online]. Available: https://commons.wikimedia.org/wiki/File:Activated_Sludge_1.svg.

[3] F. Nejjari, E. Dahhou, A. Benhammou and G. Roux, "Non-linear multivariable adaptive control of an Activated Sludge Wasterwater Treatment Process," *International Journal of Adaptive Control and Signal Processing,* vol. 13, no. 5, pp. 347-365, 1999.

[4] I. Muntean, R. Both, R. Crisan and I. Nascu, "RGA analysis and decentralized control for a wastewater treatment plant," in *IEEE International Conference on Industrial Technology (ICIT)*, Seville, 2015.

[5] R. Vilanova, R. Katebi and V. Alfaro, "Multi-loop PI-based control strategies for the Activated Sludge Process," in *IEEE Conference on Emerging Technologies & Factory Automation*, Mallorca, 2009.

[6] N. A. Wahab, M. R. Katebi and J. Balderud, "Multivariable PID control design for wastewater systems," in *Mediterranean Conference on Control & Automation*, Athens, 2007.

[7] M. Razali, N. A. Wahab, P. Balaguer, M. F. Rahmat and S. I. Samsudin, "Multivariable PID controllers for dynamic process," in *9th Asian Control Conference (ASCC)*, Istanbul, 2013.

[8] A. Chirosca, G. Ifrim, A. Filipescu and S. Caraman, "Multivariable h infinite control of wastewater biological treatment processes," *Journal of Control Engineering and Applied Informatics*, vol. 15, no. 1, pp. 11-21, 2013.

[9] X. Qiao, F. Luo and Y. Xu, "Robust PID controller design using genetic algorithm for wastewater treatment process," in *IEEE Advanced Information Management, Communicates, Electronic and Automation Control Conference (IMCEC)*, Xi'an, 2016.

[10] S. P. Bhattacharyya, A. Datta and L. H. Keel, Linear Control Theory: Structure , Robustness and Optimization, CRC Press, 2009.

[11] I. D. Díaz-Rodríguez and S. P. Bhattacharyya, "PI controller design in the achievable gain-phase margin plane," in *IEEE 55th Conference on Decision and Control (CDC)*, Las Vegas, 2016.

[12] I. D. Díaz-Rodríguez, S. Han, L. Keel and S. Bhattacharyya, "Advanced Tuning for Ziegler-Nichols Plants," *IFAC-PapersOnLine*, vol. 50, no. 1, pp. 1805-1810, 2017.

[13] G. Olsson, "State of the Art in Sewage Treatment Plant Control," Department of Automatic Control, Lund Institute of Technology (LTH), Lund, 1976.

[14] S. Skogestad and I. Postlethwaite, "Control Structure Design," in *Multivariable Feedback Control : Analysis and design*, Wiley-Interscience, 2001, pp. 405-458.

[15] E. Bristol, "On a new measure of interaction for multivariable process control," *IEEE Transactions on Automatic Control,* vol. 11, no. 1, pp. 133-134, 1966.

[16] P. Georgieva and S. F. D. Azevedo, "Robust Control Design of an Activated Sludge Process," *International Journal of Robust and Nonlinear Control,* vol. 9, no. 13, pp. 949-967, 1999.

[17] L. Åmand, G. Olsson and B. Carlsson, "Aeration control – a review," *Water Science & Technology,* vol. 67, no. 11, pp. 2374-2398, 2013.

[18] J. Maciejowski, Multivariable Feedback Design, Addison-Wesley, 1989.

[19] A. MacFarlane and B. Kouvaritakis, "A design technique for linear multivariable," *International Journal of Control,* vol. 25, no. 6, pp. 837-874, 1977.

APPENDIX A

Calculation of Stabilizing Set for G_{11}

We have G_{11} and the controller C_s defined as:

$$G_{11} = \frac{N(s)}{D(s)} = \frac{157.8\,s^3 + 303.6\,s^2 + 46.75\,s + 0.3591}{s^4 + 2.312\,s^3 + 1.021\,s^2 + 0.1135\,s + 0.0006816}$$

$$C_s(s) = \frac{K_d s^2 + K_p\, s + K_i}{s(1 + s\,)}$$

For G_{11}, $n = 4$ and $m = 3$ and $z^+ = 0$.

The closed loop characteristic polynomial is now given as:

$$\delta(s) = \left(K_d s^2 + K_p\, s + K_i\right)N(s) + s(1 + s)D(s)$$

$$\delta(s) = \left(K_d s^2 + K_p\, s + K_i\right)(157.8\,s^3 + 303.6\,s^2 + 46.75\,s + 0.3591) + s(1 + s)(s^4 + 2.312\,s^3 + 1.021\,s^2 + 0.1135\,s + 0.0006816)$$

Now we define the polynomial,

$$\nu(s) = \delta(s)N(-s)$$

$$\nu(s) = \left(K_d s^2 + K_p\, s + K_i\right)N(s)N(-s) + s(1 + s)D(s)N(-s)$$

$$\nu(s) = \left(K_d s^2 + K_p\, s + K_i\right)(-24896.7s^6 + 77393.4s^4 - 1967.43s^2 + 0.12892) + (s + s^2)(-157.78s^7 - 61.281s^6 + 494.02s^5 + 184.34s^4 - 12.566s^3 - 4.7318s^2 + 0.008886s + 0.00024472)$$

$$\nu(s) = \left(K_d s^2 + K_p\, s + K_i\right)(-24896.7s^6 + 77393.4s^4 - 1967.43s^2 + 0.12892)$$
$$+ (-157.78s^9 - 219.07s^8 + 432.74s^7 + 678.37s^6 + 171.78s^5$$
$$- 17.29s^4 - 4.7229s^3 + 0.0091307s^2 + 0.00024472s)$$

Now separating even and odd parts:

$$\nu(s) = [(-219.07s^8 + 678.37s^6 - 17.29s^4 + 0.0091307s^2)$$
$$+ (K_d s^2 + K_i)(-24896.7s^6 + 77393.4s^4 - 1967.43s^2 + 0.12892)]$$
$$+ s[(-157.78s^8 + 432.74s^6 + 171.78s^4 - 4.7229s^2 + 0.00024472)$$
$$+ K_p(-24896.7s^6 + 77393.4s^4 - 1967.43s^2 + 0.12892)]$$

And,

$$\nu(j\omega, K_p, K_i, K_d)$$
$$= [(-219.07\omega^8 - 678.37\omega^6 - 17.29\omega^4 - 0.0091307\omega^2)$$
$$+ (K_i - K_d\omega^2)(24896.7\omega^6 + 77393.4\omega^4 + 1967.43\omega^2 + 0.12892)]$$
$$+ j[(-157.78\omega^9 - 432.74\omega^7 + 171.78\omega^5 + 4.7229\omega^3$$
$$+ 0.00024472\omega) + K_p(24896.7\omega^7 + 77393.4\omega^5 + 1967.43\omega^3$$
$$+ 0.12892\omega)]$$

$$\nu(j\omega, K_p, K_i, K_d) = [p_1(\omega) + (K_i - K_d\omega^2)p_2(\omega)] + j[q_1(\omega) + K_p q_2(\omega)]$$

Where,

$$p_1(\omega) = -219.07\omega^8 - 678.37\omega^6 - 17.29\omega^4 - 0.0091307\omega^2$$

$$p_2(\omega) = 24896.7\omega^6 + 77393.4\omega^4 + 1967.43\omega^2 + 0.12892$$

$$q_1(\omega) = -157.78\omega^9 - 432.74\omega^7 + 171.78\omega^5 + 4.7229\omega^3 + 0.00024472\omega$$

$$q_2(\omega) = 24896.7\omega^7 + 77393.4\omega^5 + 1967.43\omega^3 + 0.12892\omega$$

It is required for stability that:

$$\sigma(\nu) = n - m + 2 + 2z^+ = 4 - 3 + 2 + 0 = 3$$

Since, the degree of $\nu(s)$ is odd, we see from signature formulas that odd part must have at least one positive real root of odd multiplicity. The range of K_p for this case is found to be:

$$q(\omega, K_p) = q_1(\omega) + K_p q_2(\omega) = 0$$

$$K_p = \frac{-q_1(\omega)}{q_2(\omega)}$$

The range of K_p such that $q(\omega, K_p)$ shown in figure A.1 has at least 1 positive real root of odd multiplicity was determined to be $(-0.02, \infty)$.

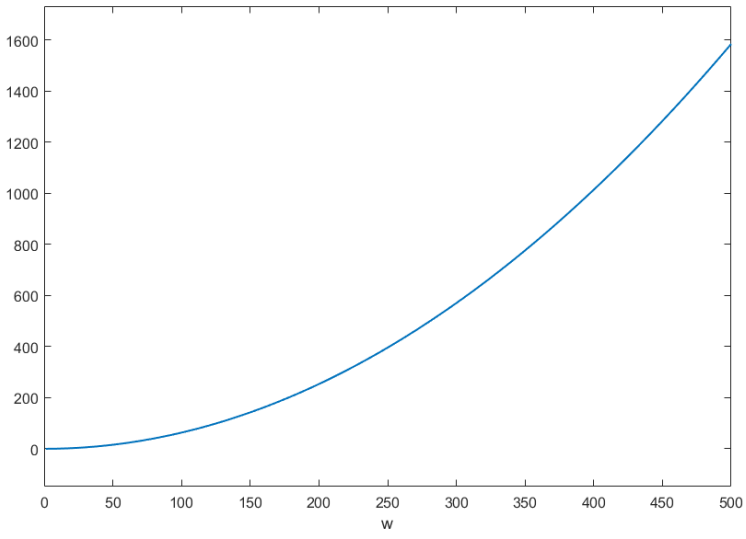

Figure A. 1. Allowable Range for Kp

For a fixed $K_p = 0.03$ in this range we have

$$q(\omega, 0.03) = q_1(\omega) + 0.03q_2(\omega)$$

$$q(\omega, 0.03) = -157.78\omega^9 + 314.13\omega^7 + 2493.58\omega^5 + 63.74\omega^3 + 0.0042\omega$$

The real, non-negative, distinct finite roots of $q(\omega, 0.03)$ with odd multiplicities are

$$\omega_0 = 0 \qquad \omega_1 = 2.25903$$

Also defining $\omega_2 = \infty$.Since

$$sgn[q(0,0.03)] = 1$$

It follows that every admissible string

$$I = \{i_0, i_1, i_2\}$$

Must satisfy

$$\{i_0 - 2i_1\}.(1) = 3$$

Hence, the admissible strings are

$$I_1 = \{1, -1\}$$

For I_1 it follows that the stabilizing set (K_i, K_d) values corresponding to $K_p = 0.03$ must satisfy the string of inequalities:

$$p_1(\omega_0) + (K_i - K_d\omega_0^2)p_2(\omega_0) > 0$$

$$p_1(\omega_1) + (K_i - K_d\omega_1^2)p_2(\omega_1) < 0$$

Substituting values fort ω_0 , ω_1 in the above expressions, we obtain,

$$K_i > 0$$

$$K_i - 5.1032K_d < -0.0448$$

The set defined by inequalities is shown in figure A.2

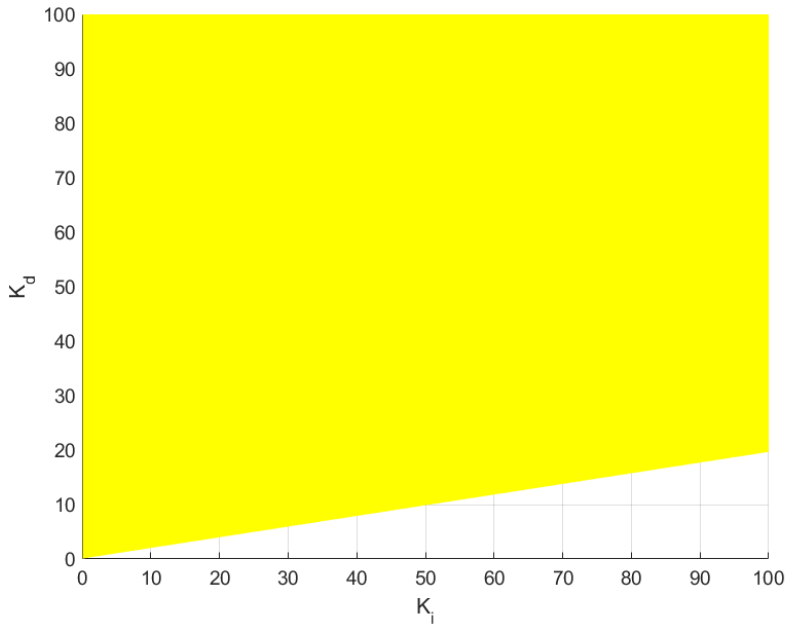

Figure A. 2. Stabilizing Set in Ki and Kd for fixed Kp = 0.03

Prescribing Stability Margins

Let $G_{11}(s)$ and $C_s(s)$ denote the plant and controller transfer functions. The frequency response of the plant and controller are $G_{11}(j\omega)$ and $C_s(j\omega)$ respectively, for $\omega \in [0, \infty]$.

$$C_s(j\omega) = \frac{K_d(j\omega)^2 + K_p\,(j\omega) + K_i}{j\omega(1 + j\omega\,)}$$

$$|C_s(j\omega)|^2 = \left(\frac{K_p}{\omega^2+1} - \frac{K_i}{\omega^2+1} + \frac{K_d\omega^2}{\omega^2+1} \right)^2 + \left(\frac{-K_p\omega}{\omega^2+1} - \frac{K_i}{\omega(\omega^2+1)} + \frac{K_d\omega}{\omega^2+1} \right)^2$$

$$\angle C_s(j\omega) = \frac{-K_p\omega^2 - K_i + K_d\omega^2}{\omega\left(K_p - K_i + K_d\omega^2\right)}$$

Now we want to prescribe Phase Margin of 60° at $\omega_g = 2\ rad/hour$.

$$\left|G_{11}(j\omega_g)\right| = 77.25$$

$$\angle G_{11}(j\omega_g) = -79.196°$$

Therefore, we have

$$\left|C_s(j\omega_g)\right| = \frac{1}{\left|G_{11}(j\omega_g)\right|} = 0.0129$$

$$\phi_g = \pi + pm - \angle G_{11}(j\omega_g) = 319.196$$

Must satisfy

$$\left(\frac{K_p}{\omega^2+1} - \frac{K_i}{\omega^2+1} + \frac{K_d\omega^2}{\omega^2+1}\right)^2 + \left(\frac{-K_p\omega}{\omega^2+1} - \frac{K_i}{\omega(\omega^2+1)} + \frac{K_d\omega}{\omega^2+1}\right)^2 = (0.0129)^2$$

$$\frac{-K_p\omega^2 - K_i + K_d\omega^2}{\omega\left(K_p - K_i + K_d\omega^2\right)} = \tan(319.196)$$

These two equations will give constant gain loci cylinder and constant phase loci plane. If their intersection lies in the stabilizing set, then the design specification is achieved.

Suppose we fix $K_d = 0.00806$, then the loci become an ellipse and a straight line respectively. We see that for stabilizing set with fixed K_d and the specifications, the design specifications can be achieved as the intersection point lies in the stabilizing set.

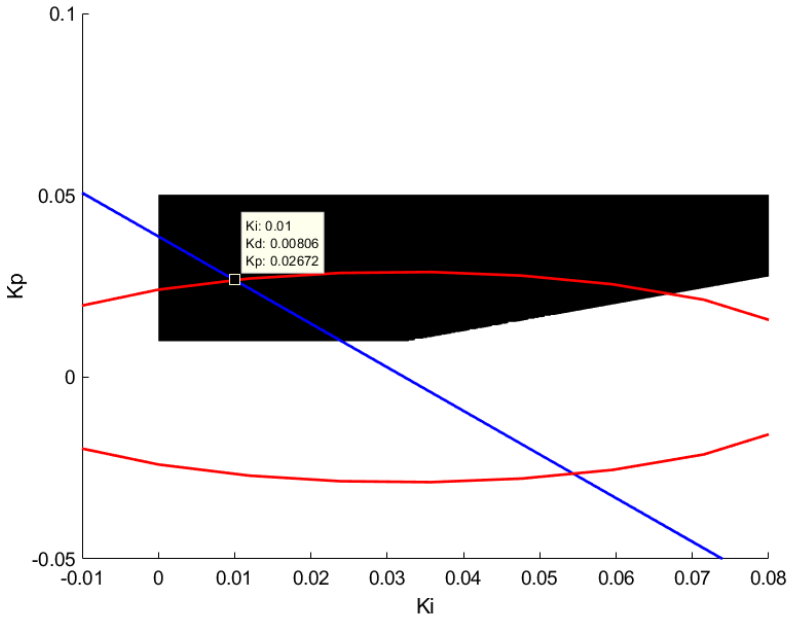

Figure A. 3. Intersection of loci and stabilizing set to find design point

Hence the designed controller for $G_{11}(s)$ which achieves $PM = 60°$ at $\omega_g = 2\ rad/hour$ is

$$C_s(s) = \frac{0.00806s^2 + 0.02672s + 0.01}{s(1+s)}$$

The GM achieved for this design point is ∞.

Calculation of Stabilizing Set for G_{22}

We have G_{11} and the controller C_{DO} defined as:

$$G_{22} = \frac{N(s)}{D(s)} = \frac{0.06725s^3 + 0.0391s^2 + 0.00476s + 2.85 * 10^{-5}}{s^4 + 2.312s^3 + 1.021s^2 + 0.1135s + 0.0006816}$$

$$C_{DO}(s) = \frac{K_d s^2 + K_p\, s + K_i}{s(1 + s\,)}$$

For G_{22}, $n = 4$ and $m = 3$ and $z^+ = 0$.

The closed loop characteristic polynomial is now given as:

$$\delta(s) = \left(K_d s^2 + K_p\, s + K_i\right)N(s) + s(1 + s)D(s)$$

$$\delta(s) = \left(K_d s^2 + K_p\, s + K_i\right)(0.06725s^3 + 0.0391s^2 + 0.00476s + 2.85 * 10^{-5}) + s(1 + s)(s^4 + 2.312s^3 + 1.021s^2 + 0.1135s + 0.0006816)$$

Now we define the polynomial,

$$\nu(s) = \delta(s)N(-s)$$

$$\nu(s) = \left(K_d s^2 + K_p\, s + K_i\right)N(s)N(-s) + s(1 + s)D(s)N(-s)$$

$$\nu(s) = \left(K_d s^2 + K_p\, s + K_i\right)(-0.00452s^6 + 0.00088s^4 - 0.0000204s^2 + 8.1 * 10^{-10}) + (s + s^2)(-0.06725s^7 - 0.1164s^6 + 0.01697s^5 + 0.02132s^4 - 0.000401s^3 - 0.000484s^2 - 8.3889 * 10^{-9}s + 1.942 * 10^{-8})$$

$$\nu(s) = \left(K_d s^2 + K_p\, s + K_i\right)(-0.00452s^6 + 0.00088s^4 - 0.0000204s^2 + 8.1 * 10^{-10}) + (-0.06725s^9 - 0.18365s^8 - 0.09943s^7 + 0.0383s^6 + 0.02092s^5 - 0.00088s^4 - 0.000484s^3 + 1.103 * 10^{-8}s^2 + 1.94 * 10^{-8}s)$$

Now separating even and odd parts:

$$\nu(s) = [(-0.18365s^8 + 0.0383s^6 - 0.00088s^4 + 1.103 * 10^{-8}s^2) + (K_d s^2 + K_i)(-0.00452s^6 + 0.00088s^4 - 0.0000204s^2 + 8.1 * 10^{-10})] + s[(-0.06725s^8 - 0.09943s^6 + 0.02092s^4 - 0.000484s^2 + 1.94 * 10^{-8}) + K_p(-0.00452s^6 + 0.00088s^4 - 0.0000204s^2 + 8.1 * 10^{-10})]$$

And,

$$\nu(j\omega, K_p, K_i, K_d) = [(-0.18365\omega^8 - 0.0383\omega^6 - 0.00088\omega^4 - 1.103 * 10^{-8}\omega^2) + (-K_d\omega^2 + K_i)(0.00452\omega^6 + 0.00088\omega^4 + 0.0000204\omega^2 + 8.1 * 10^{-10})] + j[(-0.06725\omega^9 + 0.09943\omega^7 + 0.02092\omega^5 + 0.000484\omega^3 + 1.94 * 10^{-8}\omega) + K_p(0.00452\omega^7 + 0.00088\omega^5 + 0.0000204\omega^3 + 8.1 * 10^{-10}\omega)]$$

$$\nu(j\omega, K_p, K_i, K_d) = [p_1(\omega) + (K_i - K_d\omega^2)p_2(\omega)] + j[q_1(\omega) + K_p q_2(\omega)]$$

Where,

$$p_1(\omega) = -0.18365\omega^8 - 0.0383\omega^6 - 0.00088\omega^4 - 1.103 * 10^{-8}\omega^2$$

$$p_2(\omega) = 0.00452\omega^6 + 0.00088\omega^4 + 0.0000204\omega^2 + 8.1 * 10^{-10}$$

$$q_1(\omega) = -0.06725\omega^9 + 0.09943\omega^7 + 0.02092\omega^5 + 0.000484\omega^3 + 1.94 * 10^{-8}\omega$$

$$q_2(\omega) = 0.00452\omega^7 + 0.00088\omega^5 + 0.0000204\omega^3 + 8.1 * 10^{-10}\omega$$

It is required for stability that:

$$\sigma(\nu) = n - m + 2 + 2z^+ = 4 - 3 + 2 + 0 = 3$$

Since, the degree of $\nu(s)$ is odd we see from signature formulas that odd part must have at least one positive real root of odd multiplicity. The range of K_p for this case is found to be:

$$q(\omega, K_p) = q_1(\omega) + K_p q_2(\omega) = 0$$

$$K_p = \frac{-q_1(\omega)}{q_2(\omega)}$$

The range of K_p such that $q(\omega, K_p)$ shown in figure A.4 has at least 1 positive real root of odd multiplicity was determined to be $(-20, \infty)$.

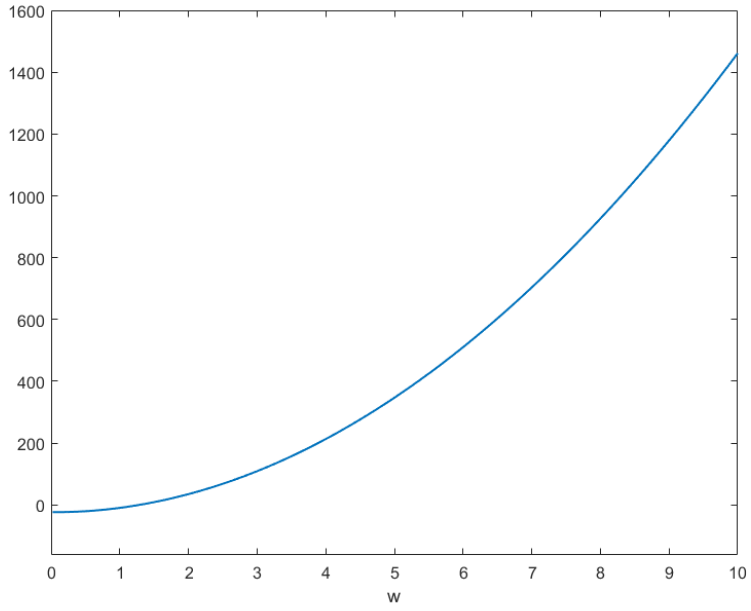

Figure A. 4. Allowable range for Kp

For a fixed $K_p = 80$ in this range we have

$$q(\omega, 80) = q_1(\omega) + 80q_2(\omega)$$

$$q(\omega, 80) = -0.06725\omega^9 + 0.4612\omega^7 + 0.09202\omega^5 + 0.002117\omega^3 + 8.44 * 10^{-8}\omega$$

The real, non-negative, distinct finite roots of $q(\omega, 80)$ with odd multiplicities are

$$\omega_0 = 0 \qquad \omega_1 = 2.655781$$

Also defining $\omega_2 = \infty$.Since

$$sgn[q(0,80)] = 1$$

It follows that every admissible string

$$I = \{i_0, i_1, i_2\}$$

Must satisfy

$$\{i_0 - 2i_1\}.(1) = 3$$

Hence, the admissible strings are

$$I_1 = \{1, -1\}$$

For I_1 it follows that the stabilizing set (K_i, K_d) values corresponding to $K_p = 80$ must satisfy the string of inequalities:

$$p_1(\omega_0) + (K_i - K_d\omega_0^2)p_2(\omega_0) > 0$$

$$p_1(\omega_1) + (K_i - K_d\omega_1^2)p_2(\omega_1) < 0$$

Substituting values fort ω_0 , ω_1 in the above expressions, we obtain,

$$K_i > 0$$

$$K_i - 7.05318K_d < 286.8904$$

The set defined by inequalities is shown in fig

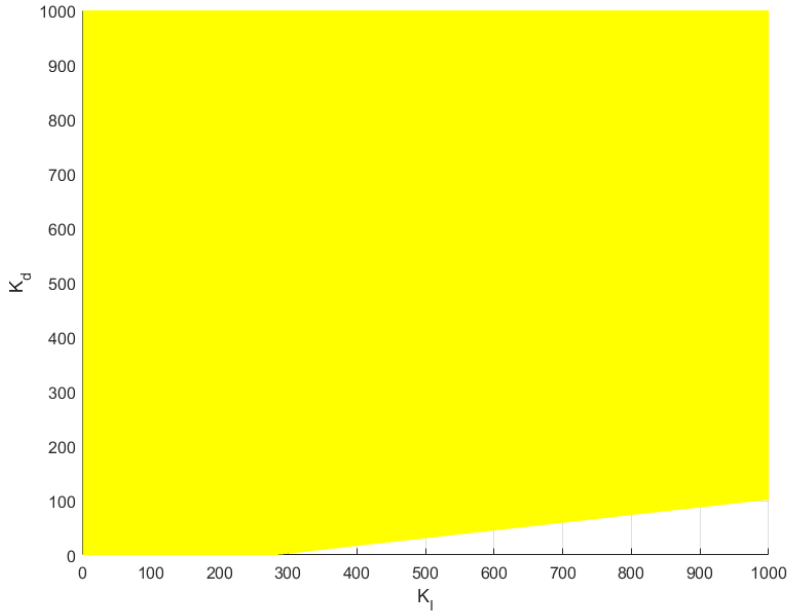

Figure A. 5. Stabilizing Set in Ki and Kd for fixed Kp = 80

Prescribing Stability Margins

Let $G_{22}(s)$ and $C_{DO}(s)$ denote the plant and controller transfer functions. The frequency response of the plant and controller are $G_{22}(j\omega)$ and $C_{DO}(j\omega)$ respectively, for $\omega \in [0, \infty]$.

$$C_{DO}(j\omega) = \frac{K_d(j\omega)^2 + K_p\,(j\omega) + K_i}{j\omega(1 + j\omega)}$$

$$|C_{DO}(j\omega)|^2 = \left(\frac{K_p}{\omega^2+1} - \frac{K_i}{\omega^2+1} + \frac{K_d\omega^2}{\omega^2+1} \right)^2 + \left(\frac{-K_p\omega}{\omega^2+1} - \frac{K_i}{\omega(\omega^2+1)} + \frac{K_d\omega}{\omega^2+1} \right)^2$$

$$\angle C_{DO}(j\omega) = \frac{-K_p\omega^2 - K_i + K_d\omega^2}{\omega\left(K_p - K_i + K_d\omega^2\right)}$$

Now we want to prescribe Phase Margin of 60° at $\omega_g = 2\ rad/hour$.

$$\left|G_{22}(j\omega_g)\right| = 0.025265$$

$$\angle G_{22}(j\omega_g) = -49.593°$$

Therefore, we have

$$\left|C_{DO}(j\omega_g)\right| = \frac{1}{\left|G_{22}(j\omega_g)\right|} = 39.5792$$

$$\phi_g = \pi + pm - \angle G_{11}(j\omega_g) = 289.593$$

Must satisfy

$$\left(\frac{K_p}{\omega^2+1} - \frac{K_i}{\omega^2+1} + \frac{K_d\omega^2}{\omega^2+1}\right)^2 + \left(\frac{-K_p\omega}{\omega^2+1} - \frac{K_i}{\omega(\omega^2+1)} + \frac{K_d\omega}{\omega^2+1}\right)^2 = (39.5792)^2$$

$$\frac{-K_p\omega^2 - K_i + K_d\omega^2}{\omega(K_p - K_i + K_d\omega^2)} = \tan(289.593)$$

These two equations will give constant gain loci cylinder and constant phase loci plane. If their intersection lies in the stabilizing set, then the design specification is achieved.

Suppose we fix $K_d = 0.2$, then the loci become ellipse and straight line respectively. We see that for stabilizing set with fixed K_d and the specifications, the design specifications can be achieved as the intersection point lies in the stabilizing set.

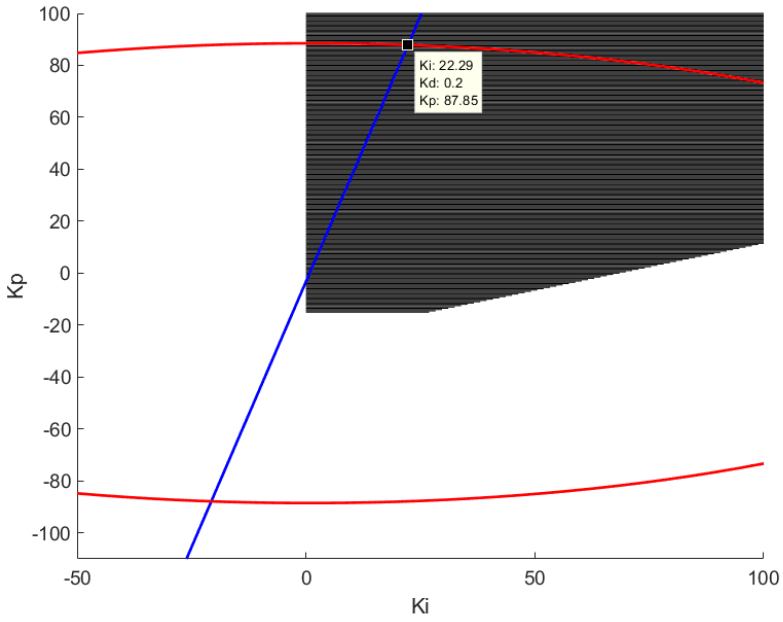

Figure A. 6. Intersection of loci and stabilizing set to find design point

Hence the designed controller for $G_{22}(s)$ which achieves $PM = 60°$ at $\omega_g = 2\ rad/hour$ is

$$C_{DO}(s) = \frac{0.2s^2 + 87.85s + 22.29}{s(1+s)}$$

The GM achieved for this design point is ∞.

APPENDIX B

This section contains MATLAB code to calculate closed loop stabilizing set for a transfer function with PID controller.

```
clc
clear

syms s
syms w kp ki kd real

%define Transfer function numerator and denominator
N = [157.7838 303.555 46.748 0.3590];
D = [1.0 2.31 1.02117 0.1134 0.00068156];

m = length(N)-1 ;
n = length(D)-1 ;
z = roots(N);
zp = length(z(z>0));
Ns = poly2sym(N,s);
Ds = poly2sym(D,s);


delta_s = s*(1+s)*Ds + (kp*s+ki+kd*s^2)*Ns; %characteristic equation
Nc = subs(Ns,s,-s);                  %N(-s)
nu = delta_s*Nc;
nu2 = subs(nu,s,1i*w);

sig_nu = n-m+2+2*zp;                %signature requirement for nu(s)

nu_real = real(nu2);
nu_im = imag(nu2);


pw = coeffs(nu_real,[ki,kd]);
pw = expand(pw)
pw = vpa(pw,5)
qw = coeffs(nu_im,kp);
qw = expand(qw)
```

```
figure()
ezplot(-(qw(1))/qw(2),[0 5]);       %find range for Kp


for kp = 0.003:0.01:0.2

    qw2 = qw(1) + kp*qw(2);
    r = roots(sym2poly(qw2))

    wr = unique(r(r>=0));
    for i = 1:length(wr)
       if(isreal(wr(i)))
          wt = wr(i);
    end
    wl = [0;wt]
    end
    J = sign(subs(qw2,w,1e-10))
    L = length(wl)

    a = [-1 1];
    b = [-1 1];
    ab = [a b];
    allcombs = nchoosek(ab, 2);
    combs = unique(allcombs, 'rows')

    ic = [1,-2]
    combs2 = combs.*ic;
    c = sum(combs2,2);

    I = combs(J*c== sig_nu,:)

    A = zeros(2,3);
    B = zeros(2,1);

    %define inequalities and plot stabilizing set
    for k = 2:length(wl)

       p1 = subs(pw(1),w,wl(k));
       p2 = subs(vpa(pw(end),4),w,wl(k));
       A = [1 0 1;-1 wl(k)^2 -1];
       B = [0+kp;(p1/p2)-kp];
       figure(2)
       plotregion(real(A),double(B), [0 0 kp], [20 20 kp],'y');
```

```
        hold on
        xlabel('Ki');
        ylabel('Kd');
        zlabel('Kp');
        grid on


    end
end
hold on

clear k i
 P = tf(N,D)

syms kp ki kd w real

C = ((i*w)*(kp)+ ki + ((i*w)^2)*kd)/(i*w*(i*w+1));

re = real(C);
im = imag(C);

setf = [];
k = 1;

%set specifications and find values of controller gains for the same
for wg = 2
    set = [];
    j = 1;
    re = real(C);
    im = imag(C);
    re = subs(re,w,wg);
    im = subs(im,w,wg);
    for pm = 60
    [mag,phase] = bode(P,wg);
    M = 1/mag
    phi = 180+pm-phase
    phirad = degtorad(phi);
    A = re^2 + im^2  == M^2
    B = (im/re) == tan(phirad)
    st = [];

for ki = 0.01:0.01:0.1

    A2 = eval(A);
```

```
    B2 = eval(B);
    sol = solve(A2,B2,'PrincipalValue',true);
    kp_sol = vpa(sol.kp);
    kd_sol = vpa(sol.kd);
temp = [kd_sol;kp_sol;ki];
    st = [st temp];
end
   set(:,:,j) = st;
plot3(set(3,:),set(1,:),set(2,:),'r*')
   hold on
  j = j+1;
syms kp ki kd
s1 = solve(A,kp);
s2 = solve(B,kp);
    syms x y z
    s1 = subs(s1,{ki,kd},{x,y});
    s2 = subs(s2,{ki,kd},{x,y});
    s3 = solve(s1(2)==s2,x);
    s4 = solve(s1(2)==s2,y);
    s5 = solve(A,ki);
    s5 = subs(s5,{kd,kp},{y,z});
    s6 = solve(B,ki);
    s6 = subs(s6,{kd,kp},{y,z});
    s7 = solve(s5(1) == s6,z);
fsurf(s1,[0 2 0 0.1])
hold on
fsurf(s2,[0 2 0 0.1])
hold on
fplot3(x,s4,s7,[0 0.5],'r','LineWidth',4)
xlim([0 0.5])
ylim([0 0.1])
zlim([0 0.04])
hold on
    end
      setf(:,:,:,k) = set;
   k = k+1;
end
```